increased E^0 from the g-position propionate involved in the hydrogen bonding to Ser 64. Therefore, the g-position propionate is only slightly more effective (by ~15 mV) than the f-position propionate in raising E^0, and this argues directly against the uniquely oriented 7-propionate of native cytochrome b_5 as providing an important stabilizing interaction for the oxidized protein.

The above conclusions are further supported by the effect on reduction potential for the symmetric hemins with variable length carboxylate side chains. Shortening the carboxylate side chains to acetates (hemin **1K**) should prevent the g-position group from being oriented to bring the carboxylate group as close to the iron as with propionate side chains with hemin **1H**. The reduction potentials for these two protein complexes, however, are indistinguishable (ca. -83 and ca. -85 mV, respectively). When the carboxylate chains are lengthened to butyrates (hemin **1J**), the 7-carboxyl side chain could get closer to the iron than a propionate (hemin **1H**). Although the reduction potential is more negative (ca. -10 mV) for hemin **1J** (ca. -93 mV) than **1H** (ca. -83 mV), consistent with some minor stabilization for the ferric state, the difference is marginal and not significantly outside the experimental uncertainties.

Moving the *f*-position propionate to position *e* (hemin **1M**; E^0 ~ -77 mV) or position h (hemin **1N**, E^0 ~ -76 mV) results in only very minor changes in reduction potential relative to that for the reference protein (hemin **1H**, E^0 ~ -83 mV). Hence the exact position of a propionate, at least among those that can be accommodated by the folded protein, does not appear to be important in determining the reduction potential. However, that the influence of propionates is not simply additive is illustrated for the tripropionate hemin **1P** (E^0 ~ -68 mV), for which the reduction potential does not become more negative by ~25 mV, as might be expected on the basis of the trend for hemins **1L** → **1H**, **1M** → **1N**, but in fact becomes more positive than for a dipropionate hemin. The ineffectiveness of the third propionate side chain in altering E^0 for the cytochrome b_5 complex of hemin **1L** may be due to the fact that the e-position propionate is not ionized.

Acknowledgment. This research was supported by grants from the National Science Foundation (DMB-88-03611 (G.N.L.)) and the National Institutes of Health (HL-22252 (K.M.S.) and DK-31038 (F.A.W.)).

Supplementary Material Available: A figure illustrating 1D NOEs for the ferricytochrome b_5 complex of hemin **1N** (1 page). Ordering information is given on any current masthead page.

Allosteric Regulation of Conformational Enantiomerism. Bilirubin

Gisbert Puzicha, Yu-Ming Pu, and David A. Lightner*

Contribution from the Department of Chemistry, University of Nevada, Reno, Nevada 89557-0020. *Received September 21, 1990*

Abstract: (4*Z*,15*Z*)-Bilirubin IXα, the cytotoxic yellow tetrapyrrole pigment of jaundice, readily adopts either of two interconverting, enantiomeric conformations, which are stabilized through complementary intramolecular hydrogen bonding between the pyrrole and lactam N—H and C=O residues of one dipyrrinone moiety and the CO_2H group of propionic acid side chains on the second dipyrrinone. One conformational enantiomer can be destabilized relative to the other through allosteric action by judicious placement of methyl groups in the propionic acid side chains. Thus, insertion of a methyl group at the *pro-R* site on the α-carbon of the propionic acid destabilizes the *M*-chirality intramolecularly hydrogen-bonded conformational enantiomer by introducing a severe nonbonded $CH_3|CH_3$ steric interaction with a pyrrole methyl substituent. In contrast, introduction of a methyl group at the *pro-S* site destabilizes the *P*-chirality enantiomer. When resolved into enantiomers, the corresponding α-methylated derivatives of a symmetric bilirubin analogue, mesobilirubin XIIIα, gave intense, bisignate circular dichroism Cotton effects ($\Delta\epsilon_{436}^{max} = \pm 246$, $\Delta\epsilon_{392}^{max} = \mp 135$) for the long-wavelength exciton transition near 433 nm ($\epsilon_{433}^{max} = 56\,000$) measured in chloroform and $\Delta\epsilon_{425}^{max} = \pm 121$, $\Delta\epsilon_{379}^{max} = \mp 87$ in pH 7.4 phosphate buffer ($\epsilon_{418}^{max} = 46\,000$). Thus, for the first time a bilirubin has been separated into its conformational enantiomers by a forced resolution originating from internal steric effects.

Normal human metabolism produces and eliminates some 300 mg per individual per day (representing the breakdown of approximately 10^{11} red blood cells/day) of the yellow pigment of jaundice, bilirubin, which is intrinsically unexcretable and cytotoxic.[1,2] What limits the facile excretability of bilirubin is its poor solubility in water,[3] its high lipid/water partition coefficient[1] and its proclivity to form association complexes with serum albumin and other proteins[1-4]—three interrelated properties that dominate the transport and metabolism of bilirubin in vivo.[2,5] However, the interesting biologic and unusual solubility properties of the pigment do not correlate well with conventional linear and porphyrin-like structural representations (Figure 1). If bilirubin adopted such conformations, which are sterically disfavored as seen from CPK space-filled molecular models, it would be predictably polar and not lipophilic.

A unique conformation, which appears to play a central role in explaining many of the properties of bilirubin, is formed by rotating the two dipyrrinone groups about the connecting CH_2 linkage so as to generate a bent or folded shape (Figure 2) in the tetrapyrrole molecule. This is the shape of bilirubin found in X-ray crystal structures of the pigment[6a,b] and analogues in which the vinyl groups are replaced by ethyl (mesobilirubin).[6c] In this conformation, which is computed to lie at or near the global energy

(1) McDonagh, A. F.; Lightner, D. A. *Pediatrics* **1985**, *75*, 443-455.
(2) For leading references, see: Ostrow, J. D., Ed. *Bile Pigments and Jaundice*; Marcel-Dekker: New York, 1986.
(3) K_{sp} for bilirubin in water at 37 °C estimated to be ~3×10^{-15} M: Brodersen, R. in ref 2, p 158.
(4) McDonagh, A. F. In *The Porphyrins*; Dolphin, D., Ed.; Academic Press: New York, 1979; Vol. 6, pp 293-491.
(5) For leading references, see: Heirwegh, K. P. M., Brown, S. B., Eds. *Bilirubin*; CRC Press: Boca Raton, FL, 1982; Vols 1 and 2.
(6) (a) Bonnett, R.; Davies, J. E.; Hursthouse, M. B.; Sheldrick, G. M. *Proc. R. Soc. London, B* **1978**, *202*, 249-268. (b) LeBas, G.; Allegret, A.; Mauguen, Y.; DeRango, C.; Bailly, M. *Acta Crystallogr., Sect. B* **1980**, *B36*, 3007-3011. (c) Becker, W.; Sheldrick, W. S. *Acta Crystallogr., Sect. B* **1978**, *B34*, 1298-1304.

0002-7863/91/1513-3583$02.50/0 © 1991 American Chemical Society

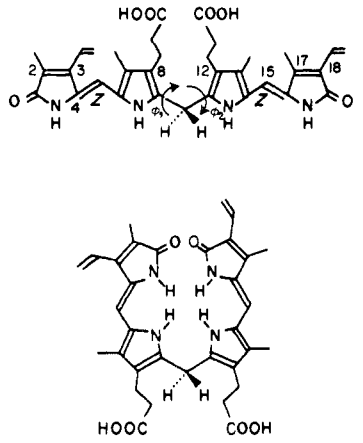

Figure 1. Linear (top) and porphyrin-like (bottom) representations for bilirubin showing two dipyrrinone chromophores conjoined by a CH_2 unit. These conformations may be interconverted through rotation of each dipyrrinone by 180° about the interconnecting CH_2, viz. about torsion angles ϕ_1 and ϕ_2.

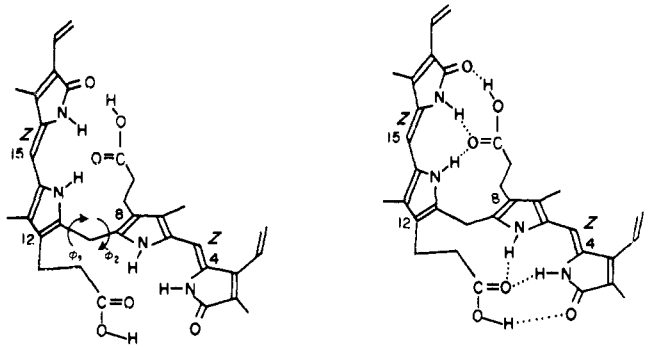

Figure 2. (Left) Folded, energy-minimum conformation of bilirubin with torsion angles $\phi_1 \simeq \phi_2 \simeq 60°$ (refs 7 and 8). The torsion angles are defined as 0° in the porphyrin-like conformation of Figure 1 and 180° in the linear representation. (Right) Folded conformation with intramolecular hydrogen bonding; the "ridge-tile" conformation found in certain crystals of bilirubin (ref 6).

minimum,[7,8] the propionic acid carboxyl groups are positioned for facile hydrogen bonding to the opposing dipyrrinone lactam C=O and N—H and pyrrole N—H groups. Considerable additional energy stabilization is obtained through such intramolecular hydrogen bonding, which leads to formation of the "ridge-tile" structures (Figure 2) seen in the crystal[6] and deduced for the pigment in solution by NMR[9,10] and circular dichroism[11] measurements.

Such ridge-tile structures adopt either of two enantiomeric conformations, which interconvert by breaking and remaking all of the hydrogen bonds (Figure 3) and rotation about torsion angles ϕ_1 and ϕ_2 (Figure 1). In chloroform solvent the rate of conformational inversion of the intramolecularly hydrogen-bonded enantiomers has been estimated independently by two different NMR methods to be 7.2 ± 0.4 (~53 °C)[9] and 3–95 s^{-1} (50–95 °C),[10] and the activation barrier for interconversion has been

Scheme I

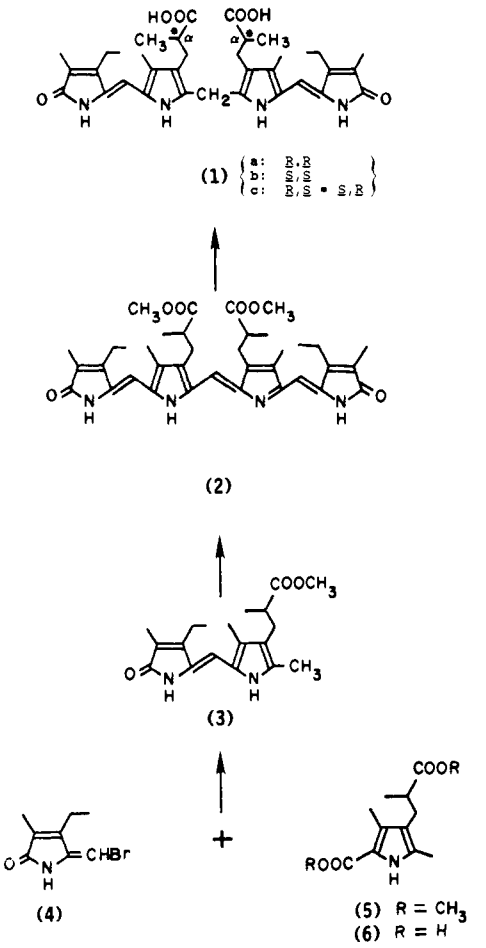

determined to be ~18 kcal/mol.[9,10] In solutions of bilirubin the enantiomeric equilibrium can be displaced toward one enantiomer through the addition of an optically active amine[11,12] or a protein,[12,13] and the net optical activity of the pigment can be detected and measured by circular dichroism (CD) spectroscopy. The largest Cotton effect magnitudes, which approach the calculated theoretical maximum ($|\Delta\epsilon| \simeq 270$ L·mol^{-1}·cm^{-1}),[11] are those seen in the presence of certain serum albumins ($|\Delta\epsilon| \simeq 250$ L·mol^{-1}·cm^{-1} for porcine serum albumin in aqueous buffer)[14] and certain amines ($|\Delta\epsilon| \simeq 210$ L·mol^{-1}·cm^{-1} for (−)-ψ-ephedrine methyl ether in benzene).[15] However, whether these particularly large $\Delta\epsilon$ values can be attributed to complete displacement of the conformational equilibrium toward one enantiomer is unconfirmed because no one has ever resolved bilirubin into its enantiomers and measured their CD spectra. In the following we report on the synthesis of diastereomeric bilirubin analogues (**1**, Figure 4), some of which can easily adopt well-defined bilirubin conformations. The racemic diastereomer (**1a** + **1b**) should in principle, be separable and resolvable into enantiomers. Each (*R,R* or *S,S*) enantiomer can adopt only one of the intramolecularly hydrogen-bonded and folded (enantiomeric) conformations, as dictated by the allosteric action of methyl substitution in the propionic acid side chains, and each is expected to show very intense bisignate CD spectra. Because a significant $CH_3|CH_3$ nonbonding steric interaction can exert itself only in folded, intramolecularly hydrogen bonded conformations, the results of the present work will also confirm for the first time importance of such hydrogen-bonded conformation in a variety of solvents, even in water at alkaline

(7) Person, R. V.; Lightner, D. A., unpublished. Molecular mechanics calculations indicate a global minimum for the (folded) conformation with $\phi_1 \simeq \phi_2 \simeq 62°$ (where ϕ_1 and ϕ_2 are defined as 0° in the porphyrin-like conformation of Figure 1). Intramolecular hydrogen bonding is computed to lower the total energy of the folded conformation by an additional 16 kcal/mol.

(8) Falk, H. *The Chemistry of Linear Oligopyrroles and Bile Pigments*; Springer Verlag: New York, 1989.

(9) Manitto, P.; Monti, D. *J. Chem. Soc., Chem. Commun.* **1976**, 122–123.

(10) (a) Kaplan, D.; Navon, G. *Isr. J. Chem.* **1983**, *23*, 177–186. (b) Kaplan, D.; Navon, G. *Biochem. J.* **1982**, *201*, 605–613. (c) Navon, G.; Frank, S.; Kaplan, D. *J. Chem. Soc., Perkin Trans. 2* **1984**, 1145–1149.

(11) Lightner, D. A.; Gawroński, J.; Wijekoon, W. M. D. *J. Am. Chem. Soc.* **1987**, *109*, 6354–6362.

(12) For leading references, see: Lightner, D. A.; Wijekoon, W. M. D.; Zhang, M.-H. *J. Biol. Chem.* **1988**, *263*, 16669–16676.

(13) Blauer, G. *Isr. J. Chem.* **1983**, *23*, 201–209, and references therein.

(14) Harmatz, D.; Blauer, G. *Arch. Biochem. Biophys.* **1975**, *170*, 375–386.

(15) Pu, Y.-M.; Lightner, D. A. *Croat. Chem. Acta* **1989**, *62*, 301–324.

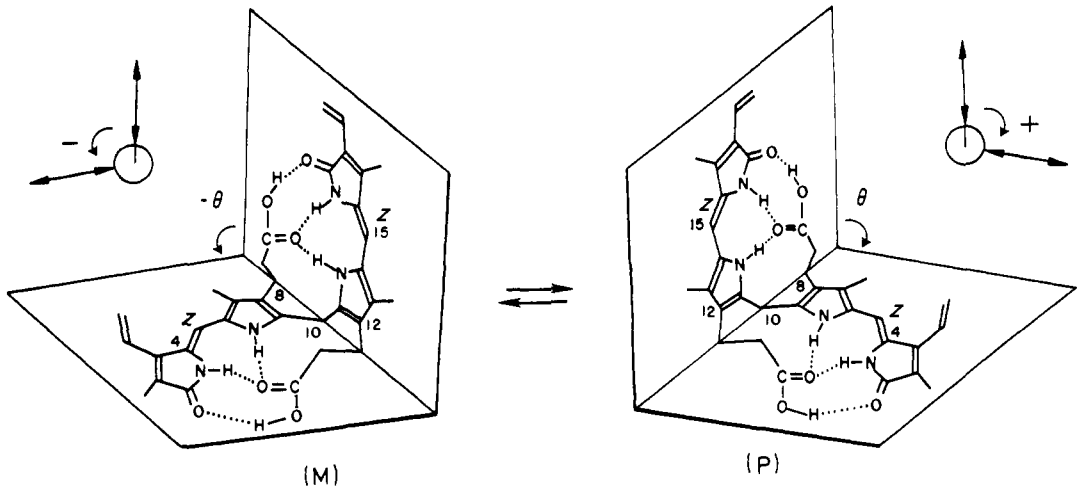

Figure 3. Interconverting enantiomeric conformers of intramolecularly hydrogen bonded bilirubin. The interplanar angle between the two planar dipyrrinone chromophores is defined as θ, and the chirality of their respective electric dipole transition moments (shown by double-headed arrows and passing lengthwise through the chromophores) is defined as *M* (minus chirality) or *P* (plus chirality).

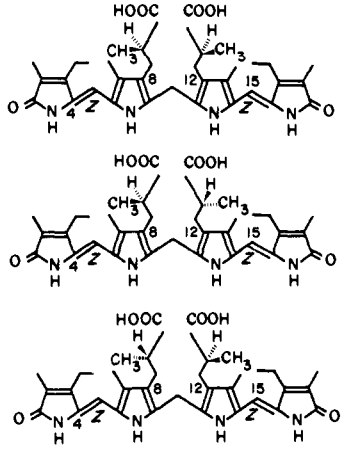

Figure 4. Linear representations for the enantiomeric and diastereomeric α,α'-dimethyl derivatives of mesobilirubin XIIIα: top, *R,S*; middle, *R,R*; bottom, *S,S*.

pH, where hydrogen bonding is thought to be reduced. These results are significant for they define and relate experimentally the chirality of pigment conformation of the CD spectra, they confirm the importance of intramolecular hydrogen bonding to the stabilization of conformation, and they provide insights into the structure of the pigment in biological fluids and tissues.

Results and Discussion

Synthesis, Stereochemistry, and Resolution. The synthesis of **1** (Scheme I) can most easily be accomplished with appropriate modifications of previously described total syntheses of mesobilirubin XIIIα.[16,17] These employ oxidative self-coupling of xanthobilirubic acid methyl ester[18] to give mesobiliverdin XIIIα dimethyl ester[17] as the key step. For present purposes, xanthobilirubic acid methyl ester with an α-methyl group in the propionic ester side chain (**3**) is the key synthetic precursor to the diastereomeric verdin mixture **2** and hence the target mesobilirubins **1**. Dipyrrinone **3** can be prepared by coupling two pyrrole derivatives: (bromomethylene)oxopyrrole **4** and dicarboxylic acid **6**. The former (**4**) can be prepared in an overall 38% yield in four steps from ethyl acetoacetate and pentane-2,4-dione:[18] (1) Fischer–Knorr pyrrole synthesis yields 4-acetyl-3,5-dimethylpyrrole-2-carboxylic acid ethyl ester, which can be converted smoothly to kryptopyrrole (2,4-dimethyl-3-ethyl-1*H*-pyrrole) under Huang–Minlon reduction conditions. (2) Oxidation of kryptopyrrole with hydrogen peroxide yields 3,5-dimethyl-4-ethyl-1*H*,5*H*-pyrrole, which can be converted to **4** by bromination under controlled conditions. The latter (**6**) is readily obtained from the corresponding diester (**5**), which is prepared by condensing ethyl acetoacetate and methyl 4-acetyl-2-methylhexanoate by using the Fischer pyrrole synthesis. The hexanoate precursor may be prepared by a KF-catalyzed Michael condensation reaction between pentane-2,4-dione and methyl methacrylate.

Table I. Influence of Reaction Solvent on the Distribution of Verdin and Rubin Diastereomers Formed Following Self-Coupling of Racemic Dipyrrinone 3 at 0 °C

solvent	verdin 2		rubin 1	
[THF]:[DMSO]	% racemic	% meso	% racemic	% meso
100:0	80	20	85	15
90:10	80	20	85	15
80:20	70	30	75	25
50:50	62	38	65	35
20:80	62	38	65	35

It is interesting to note although that the oxidative (DDQ) self-coupling step converts dipyrrinone **3** into a mixture of diastereomeric verdins (**2**) [(*R,R* + *S,S*) + (*R,S* = *S,R*)]—as expected since racemic **3** is used—the ratio of racemic to meso diastereomers is not 1:1. Rather, the amount of racemic diastereomer [(*R,R* + *S,S*)] produced exceeds considerably (2:1–4:1) that of the meso diastereomer [(*R,S*)]. The ratio varies only moderately with changes in solvent (Table I), , a fact that apparently points to the greater stability of a racemic intermediate (vs the meso intermediate) at a reversible mechanistic step, possibly the one involving the initially formed tetrapyrrole,[16] where the potential for some intramolecular hydrogen bonding might stabilize the racemic diastereomer more than the meso diastereomer. Alternatively, a constitutional isomerization[4,16] of the newly formed (**1a** + **1b**) and **1c** might take place just before their oxidation to the verdins.

The diastereomeric mixture of mesobilirubins **1** could be separated into two fractions, either by extraction from dichloromethane into 50% saturated aqueous sodium bicarbonate or by chromatography. The more polar diastereomer extracted into bicarbonate ran more slowly on silica TLC and also ran faster on reverse-phase HPLC. We assign the stereochemistry of this diastereomer to the meso (*R,S*) isomer (**1c**) for the following reasons. In its enantiomeric, folded and intramolecularly hydrogen-bonded conformations (Figure 5), the α- and β-CH_2 hydrogens of the propionic acid chains of mesobilirubin XIIIα or bilirubin lie in different steric environments. For example, a CPK space-filled molecular model of the *M*-chirality conformer shows

(16) Trull, F. R.; Franklin, R. W.; Lightner, D. A. *J. Heterocycl. Chem.* **1987**, *24*, 1573–1579.
(17) Falk, H.; Grubmayr, K. *Synthesis* **1977**, 614–615.
(18) Lightner, D. A.; Ma, J.-S.; Adams, T. C.; Franklin, R. W.; Landen, G. L. *J. Heterocycl. Chem.* **1984**, *21*, 139–144. Shrout, D. P.; Lightner, D. A. *Synthesis*, in press.

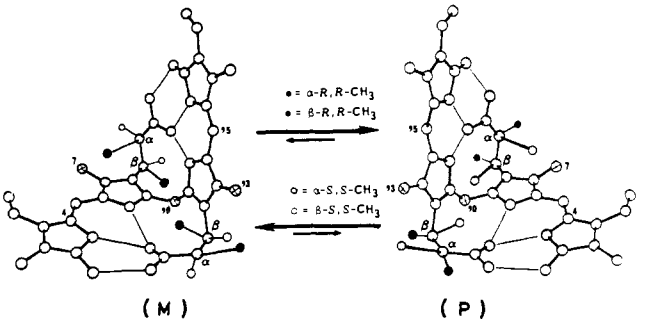

Figure 5. Ball and stick models of folded intramolecularly hydrogen bonded bilirubin (Figure 2). The smaller circles (at α and β) represent the hydrogen atoms of the propionic acid $C(\alpha)H_2$ $C(\beta)H_2$ segments. The darkened smaller filled circles are the *pro-R* hydrogens, which are sterically crowded by the C_7 and C_{13} methyl groups (⊗) or the C_{10} CH_2 (⊗) in the *M*-helicity conformation. The smaller open circles are the *pro-S* hydrogen, which are sterically crowded in the *P*-helicity conformation. Replacing α or β ● by CH_3 gives the *R,R* diastereomer and drives the equilibrium toward *P*. On the other hand, replacing α or β ○ by CH_3 gives the *S,S* diastereomer and drives it toward *M*. But replacing one α ● by CH_3 and one α ○ by CH_3 gives a meso diastereomer (*R,S*), which can adopt either the *M*- or the *P*-helicity conformation while leaving one propionic acid free and not hydrogen bonded.

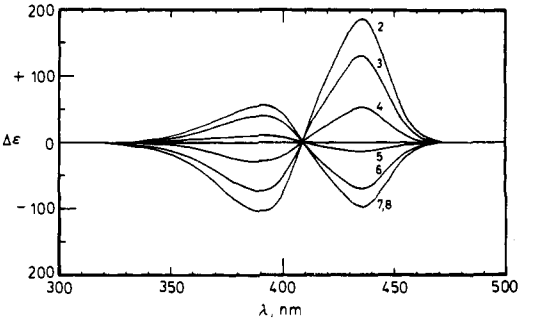

Figure 6. Bisignate circular dichroism spectra in ethanol-free chloroform of successive fractions from the resolution of racemic α,α'-dimethylmesobilirubin XIIIα (**1a** + **1b**) obtained by passing through a column of quinine covalently bound to silica gel. Fraction 1 contained no pigment. The CD of fraction 8 was the same as that of fraction 7. The CD values are given in Table V.

that the *α-pro-R* hydrogens lie very close to the methyl groups at C_7 and C_{13}; whereas, the *α-pro-S* hydrogens are much less sterically congested. In the *P*-chirality conformer the reverse can be seen: the *α-pro-S* hydrogens lie close to the methyl groups at C_7 and C_{13}; whereas, the *α-pro-R* hydrogens are uncrowded. When one of the hydrogens at the α-CH_2 group of the propionic acid chain of mesobilirubin XIIIα (Figure 4) is replaced by a methyl group, one can expect the methyl group to seek the least hindered position. Assuming that the integrity of the matrix of intramolecular hydrogen bonds is maintained, this means that a CH_3 at the *pro-R* site would direct the conformational equilibrium toward *P*, and a CH_3 at the *pro-S* site would direct it toward *M* (as shown in Figure 5 for ball and stick models). For methyl substitution in both propionic acid chains, as in **1**, the tendency toward displacing the conformational enantiomerism away from 1:1 is reinforced in the α,α'-*R,R* and α,α'-*S,S* enantiomers, which can be expected to adopt preferentially the *P*- and *M*-chirality conformations, respectively. However, when the configurations at the propionic acid α-carbons are not the same, as in the α,α'-*R,S* (meso) diastereomer, equivalent destabilizing steric interactions are introduced into both the *M* and the *P* conformational diastereomers. That is, although the methyl group of the *α-R* configuration would fit comfortably in the *P*-chirality intramolecularly hydrogen-bonded conformer, the methyl of the *α-S* would not. Similarly, although the *α-S* configuration methyl group would fit comfortably in the *M*-chirality conformer, the *α-R* methyl would not. This steric destabilization can be expected to produce conformations where at least one propionic acid group is not involved in intramolecular hydrogen bonding, thus leading to increased polarity and different solubility and chromatographic properties for the meso diastereomer (**1c**). For these reasons, we assign the α,α'-*R,S* configuration to the more polar bilirubin analogue **1c**.

The separated racemic diastereomer should in principle be resolvable into its enantiomeric components. Resolution was accomplished in two ways as described in the following. Earlier findings showed that quinine exerts a highly selective chiral recognition for bilirubin and mesobilirubin XIIIα, as seen from the intense induced CD curves for these pigments in dichloromethane solvent in the presence of cinchona alkaloids.[11] Thus we felt that quinine might prove to be a good resolving agent if immobilized on a stationary phase. Accordingly, we derivatized[19] dried silica gel with (3-mercaptopropyl)trimethylsiloxane and then covalently attached quinine through its vinyl group by means of a free radical SH addition.[20] A dichloromethane solution of the racemic α,α'-dimethylmesobilirubin XIIIα (**1a** + **1b**) was then passed through a column containing the quinine-bound silica gel, and the fractions were monitored by CD. The first eluted pigment exhibited a bisignate CD (long-wavelength positive, short-wavelength negative), as shown in Figure 6. Further elution gave fractions with bisignate CDs of reduced magnitude and then inverted signs. The final fractions had intense long-wavelength-negative, short-wavelength-positive Cotton effects. The order of elution indicates that the long wavelength negative, short wavelength positive enantiomer forms the stronger association complex with quinine, which is consistent with our earlier studies[11] showing a long-wavelength-negative, short-wavelength-positive CD for bilirubin–quinine solutions in dichlormethane. That is, quinine binds more tightly to the *M*-chirality enantiomer of bilirubin and thus displaces the $M \rightleftarrows P$ enantiomeric interconversion of Figure 3. With the racemic α,α'-dimethylmesobilirubin XIIIα (**1a** + **1b**), however, there is essentially no $M \rightleftarrows P$ interconversion, and the chiral recognition exhibited by quinine for the *M*-chirality conformer leads to resolution on the column. When the separated fractions are rechromatographed on the chiral column, further resolution is achieved, with long-wavelength $\Delta\epsilon$ values approaching ±250. Since the conformational analysis of the preceding paragraph predicts that the α,α'-*R,R* enantiomer would adopt preferentially the *P*-chirality conformational enantiomer, and the α,α'-*S,S* would adopt the *M*, we would assign the faster eluting enantiomer to the *P*-chirality, α,α'-*R,R* isomer.[11]

Resolution can be achieved in yet another way. Previously, we suggested the presence of an excess of *P*-chirality conformational enantiomer for $M \rightleftarrows P$ equilibrating bilirubin or mesobilirubin XIIIα bound to human serum albumin (HSA) in aqueous solutions prepared in the conventional way.[12] Thus, if HSA were to bind more tightly to one of the conformational enantiomers, then the remaining enantiomer might be removed selectively by extraction into, e.g., chloroform. Our preliminary attempts to resolve bilirubin into its conformational enantiomers by extraction of HSA-bound bilirubin has not yet given detectable optical activity in the extracts. The failed attempts may be attributed to our inability to retard rapid interconversion between *M* and *P* conformational enantiomers after their separation.[9,10] However, for racemic **1**, where the *M* and *P* conformational diastereomers are *not* expected to interconvert, extraction of an aqueous solution containing HSA, **1a**, and **1b** might be expected to selectively remove one enantiomer (the less tightly bound enantiomer) and thus achieve an optical resolution. In fact, the very first chloroform washing of an aqueous solution of 1:2 [HSA]:[(**1a** + **1b**)] removed pigment into chloroform, and the chloroform solution exhibited a very strong bisignate CD (Figure 7). Further washings gave pigment with progressively less intense bisignate CDs and then

(19) According to the procedure of Prof. J. F. W. Keana, University of Oregon. See also: Waddell, T. G.; Leyden, D. E.; DeBello, M. T. *J. Am. Chem. Soc.* **1981**, *103*, 5303–5307.

(20) Salvadori, P.; Rosini, C.; Pini, D.; Bertucci, C.; Altemura, P.; Uccello-Barretta, G.; Raffaelli, A. *Tetrahedron* **1987**, *43*, 4969–4978.

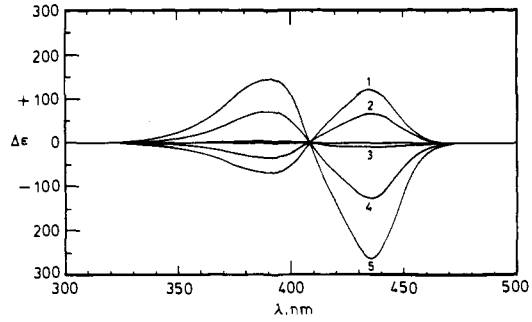

Figure 7. Bisignate circular dichroism spectra of the successive 100-mL chloroform extracts of 100 mL of an initially 1:2 mole/mole aqueous solution of human serum albumin (2.20×10^{-4} M) and bilirubin (4.35×10^{-4} M). The CD values may be found in Table VI.

sign-reversed and increasingly more intense CDs. The final washings gave an essentially optically pure sample of one enantiomer of the pigment, which could not be resolved to give larger $\Delta\epsilon$ values by reresolution. However, reresolution of the pigment (above) isolated in the first extraction of the initial resolution gave what we believe to be a nearly optically pure sample of the other enntiomer ($\Delta\epsilon_{436}^{max}$ +246, $\Delta\epsilon_{393}^{max}$ −133).

Absolute Configuration. According to exciton chirality theory,[11] we would assign the $\Delta\epsilon_{435}^{max} = -251$, $\Delta\epsilon_{391}^{max} = +142$ (chloroform) bisignate CD to the *M*-chirality conformational enantiomer with the *S,S* configuration (hence **1b**). An NMR method was used to support the assignment. Racemic **1a** + **1b** was reacted[21] with (*S*)-(−)-α-methylbenzylamine in the presence of diphenylphosphoryl azide to afford a mixture of diastereomeric bisamides, which were expected to retain the matrix of intramolecular hydrogen bonds (Figure 8) with the carboxyl O–H being replaced by the new amide N–H moiety. Interestingly, the mixture (**7a** + **7b**) gave a CD spectrum (Figure 8) in chloroform ($\Delta\epsilon_{435}^{max}$ = +60, $\Delta\epsilon_{395}^{max} = -37$) nearly identical with that of the corresponding bisamide of mesobilirubin XIIIα. ($\Delta\epsilon_{433}^{max}$ = +55, $\Delta\epsilon_{392}^{max} = -33$), whose intramolecularly hydrogen-bonded diastereomers (corresponding to **7a** and **7b**, Figure 8) are interconverting in solution.[21] Unlike the bisamide of mesobilirubin XIIIα, however, the diastereomeric bisamides of α,α′-dimethylmesobilirubin XIIIα (**7a** + **7b**) could be separated by TLC on silica gel, and the separated diastereomers did not interconvert.

Inspection of Dreiding or CPK space-filled molecular models reveals different steric environments of the C_7/C_{13} methyl groups on the pyrrole rings in the intramoleculary hydrogen-bonded conformations: They lie close to the (*S*)-amine component phenyls of the bisamide of the *R,R* acid but are much more distant from the phenyls in the bisamide of *S,S* acid. According to this picture, one might expect that irradiating the C_7/C_{13} methyls would produce a stronger NOE for the phenyl proton signals of the (*S*)-amine moiety in the bisamide of the *R,R* acid than in the bisamide of the *S,S* acid. In fact, the faster moving (TLC) diastereomer gave a 3% NOE enhancement for the phenyl proton signals; whereas, no enhancement (NOE ≪ 1%) could be found for the slower moving diastereomer. Consequently, we assign the faster moving diastereomer to the bisamide of (*R,R*)-α,α′-dimethylmesobilirubin XIIIα (**1a**). In confirmation of this assignment, the separated α,α′-dimethylmesobilirubin XIIIα enantiomer with $\Delta\epsilon_{436}^{max}$ = +246, $\Delta\epsilon_{393}^{max}$ = −133 (chloroform) was converted to its bisamide with (*S*)-(−)-α-methylbenzylamine, and this derivative was identical with the faster moving diastereomer described above and assigned by NOE experiments to the bisamide of (*S*)-(−)-methylbenzylamine of the *R,R* acid. These NMR-based assignments of absolute configuration are in complete accord with those assigned by CD and exciton chirality theory.[11]

It is interesting to note that chromatographic separation of the diastereomeric mixture of bisamides (**7a** + **7b**) effectively performs a resolution of the component enantiomeric pigments (**1a** + **1b**). And the separated diastereomers (faster moving **7a**, which is derived from **1a**, and slower moving **7b**, which is derived from **1b**) give nearly mirror image bisignate CD curves, as one might expect from intramolecular exciton systems (Figure 8). The extremely large $\Delta\epsilon$ magnitudes correspond well to folded pigment conformations,[11] and the mirror image CD curves of **7a** and **7b** indicate that the pigments have adopted enantiomeric conformations—as determined by the stereochemistry (*R,R* or *S,S*) at the α-carbon of the propionic acid amide groups. This situation can obtain only through intramolecular hydrogen bonding (Figure 8). The current investigation therefore reconfirms the presence and importance of amide N–H bonding in bilirubin derivatives of primary amines.[21]

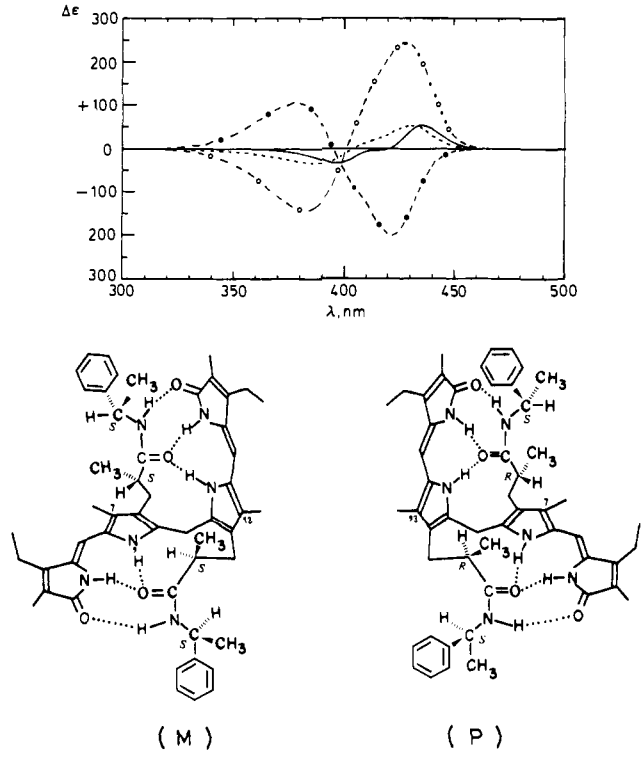

Figure 8. (Upper) Circular dichroism spectra of the bisamide (**7a** + **7b**) of racemic α,α′-dimethylmesobilirubin XIIIα (**1a** + **1b**) with (*S*)-(−)-α-methylbenzylamine (—) and of the bisamide of mesobilirubin XIIIα with the same amine (---). Circular dichroism spectra of pure **7a** (○ --- ○) and **7b** (●). The spectra were run on 2×10^{-5} M solutions in $CHCl_3$ at 21 °C. The CD data are as follows: **7a** ($\Delta\epsilon_{428}^{max}$ = +250, $\Delta\epsilon$ = 0 at λ = 401, $\Delta\epsilon_{383}^{max}$ = −140), **7b** ($\Delta\epsilon_{424}^{max}$ = −200, $\Delta\epsilon$ = 0 at λ = 395, $\Delta\epsilon_{380}^{max}$ = +110), **7a** + **7b** 1:1 ($\Delta\epsilon_{435}^{max}$ = +60, $\Delta\epsilon$ = 0 at λ = 414, $\Delta\epsilon_{395}^{max}$ = −37), and the bisamide of mesobilirubin XIIIα with (*S*)-(−)-α-methylbenzylamine ($\Delta\epsilon_{433}^{max}$ = +55, $\Delta\epsilon$ = 0 at λ = 408, $\Delta\epsilon_{392}^{max}$ = −32).

Upon closer inspection, it may be seen that the corresponding $|\Delta\epsilon|$ values of diastereomers **7a** ($\Delta\epsilon_{429}^{max}$ = +250, $\Delta\epsilon_{383}^{max}$ = −140 in $CHCl_3$) and **7b** ($\Delta\epsilon_{424}^{max}$ = −210, $\Delta\epsilon_{380}^{max}$ = +110 in $CHCl_3$) are not equal. Since the CD intensities and signs derive from exciton coupling, the differences noted indicate that the pigment conformations are not strictly mirror images. This can be attributed to differing steric environments for the amine components **7a** and **7b**. In molecular models for the former, there is little evidence of any steric interference between the *R,R* pigment and (*S*)-amine moieties, and the observed CDs of **7a** and **1a** have nearly identical $\Delta\epsilon$ values. In **7b**, however, steric interactions between the *S,S* pigment and (*S*)-amine components lead to a flattening (larger θ, Figure 3) of the pigment and a concomitant drop in $\Delta\epsilon$ values, as predicted by theory.

NMR Spectra and Structure. The ^1H NMR spectra (Table II) of (**1a** + **1b**) and **1c** show significant differences in the N*H* region in $CDCl_3$, a solvent that preserves intramolecular hydrogen bonding.[10,21] The N*H* resonances of **1a** + **1b** in $CDCl_3$ are very similar to those of mesobilirubin XIIIα, which is thought to preferentially adopt the folded, intramolecularly hydrogen-bonded conformation. But **1c** exhibits two sets of N*H* resonances: two lactam signals at 10.65 and 9.90 ppm and two pyrrole signals at

(21) Lightner, D. A.; Zhang, M. H. *Tetrahedron* **1988**, *44*, 4679–4688.

Table II. Proton NMR Spectra[a] of Racemic and Meso Diastereomers of α,α′-Dimethylmesobilirubin XIIIα in $CDCl_3$ and DMSO-d_6 Solvents at 22 °C

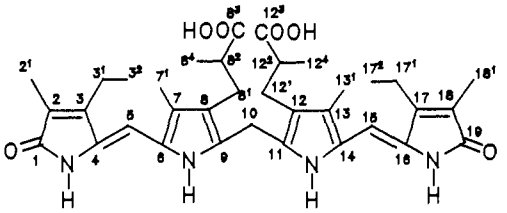

hydrogen	racemic (1a + 1b)		meso (1c)		mesobilirubin XIIIα	
	$CDCl_3$	DMSO-d_6	$CDCl_3$	DMSO-d_6	$CDCl_3$	DMSO-d_6
COOH (s)	13.68	11.95	13.77 (br)	12.04	13.31	11.88
lactam NH (s)	10.55	9.85	10.65, 9.90	9.76	10.52	9.72
pyrrole NH (s)	9.09	10.30	9.35, 9.04	10.30	9.15	10.27
C_5/C_{15} =CH (s)	6.05	5.95	6.05	5.92	6.04	5.95
C_{10} CH_2 (s)	4.04	3.95	4.06	3.98	4.06	3.97
C_2/C_{18} CH_3 (s)	1.86	1.77	1.84	1.78	1.85	1.70
C_7/C_{13} CH_3 (s)	2.15	2.00	2.15	2.02	2.14	2.06
CH_2CH_3 (t)	1.12	1.08	1.10	1.07	1.12	1.10
CH_2CH_3 (q)	2.48	2.50	2.35–2.7	2.49	2.48	2.50
α-$CHCH_3$ (d)	1.45	0.89	1.44	0.86		
$CH_AH_BCH_XCH_3$	2.42	2.05	2.35	2.30		
	J_{AB} = 14.4 Hz	J_{AB} = 13.8 Hz				
$CH_AH_BCH_XCH_3$	2.90	2.48		2.65		
	J_{BX} = 12.2 Hz					
$CH_ACH_BCH_XCH_3$	3.05	2.18	2.7	2.38		
	J_{AX} = 2.2 Hz					

[a] Values in δ, ppm downfield from $(CH_3)_4Si$ for 10^{-2} M pigment solutions.

Table III. Solvent Effects on the ^1H NMR Spectra[a] of Racemic α,α′-Dimethylmesobilirubin XIIIα (1a + 1b)

solvent	COOH	lactam NH	pyrrole NH	C_5/C_{15} =CH	C_{10} CH_2	lactam CH_3	pyrrole CH_3	CH_3CH_2	CH_3CH_2	α-CH_3	propionic CH_A-H_BCH_X	propionic CH_A-H_BCH_X	propionic CH_A-H_BCH_X	J_{AB}	J_{AX}	J_{BX}
benzene-d_6		11.07	9.58	6.10	4.11	1.82	2.11	0.93	2.16	1.41	2.41	2.98	3.15	14.4	2.8	12.2
CCl_4	13.85	10.54	9.02	5.90	3.98	1.82	2.15	1.11	2.44	1.47	2.35	2.86	2.96	13.7	1.7	12.0
CD_2Cl_2	13.82	10.52	9.07	6.08	4.04	1.83	2.15	1.10	2.49	1.45	2.43	2.91	3.04	14.0	2.4	12.2
$CDCl_3$	13.68	10.55	9.09	6.05	4.04	1.86	2.15	1.12	2.48	1.45	2.42	2.90	3.05	14.4	2.2	12.2
THF-d_8		10.45	9.10	6.13	4.06	1.81	2.16	1.10	2.52	1.44	2.44	2.93	3.04	14.0	2.0	12.0
dioxane-d_8	13.77	10.36	9.09	6.07	4.06	1.81	2.14	1.10		1.39	2.40	2.92	3.01			
pyridine-d_5		10.86	10.29	6.20	4.30	1.76	2.20	0.97	2.35	1.33	3.00	broad	2.55			
DMF-d_7[b]		10.40	9.36	6.12	4.12	1.82	2.14	1.13	2.58	1.06	2.40	2.90	2.52			
		9.73	10.27	6.15			1.97			1.12						
DMSO-d_6	11.95	9.85	10.30	5.95	3.95	1.77	2.00	1.08	2.50	0.89	2.05	2.48	2.18	13.8		

[a] Values in δ, ppm downfield from $(CH_3)_4Si$ for 10^{-2} M pigment solutions at 22 °C; J in hertz. [b] Two forms present; top:bottom = 3:1.

9.35 and 9.04 ppm. The data are consistent with partially intramolecularly hydrogen bonded conformation; that is, one with an intramolecularly hydrogen bonded dipyrrinone (δ_{NH} at 10.65 and 9.04 ppm) and a non-hydrogen-bonded (or poorly hydrogen bonded) dipyrrinone (δ_{NH} at 9.90 and 9.35 ppm)—the structure predicted by molecular models. In contrast, the chemical shifts of the C*H* hydrogens of **1a + 1b**, **1c**, and mesobilirubin XIIIα are all rather similar in $CDCl_3$, suggesting that with the α-CH_3 substitution no gross structural changes or steric compressions occur. The fact that the same chemical shifts are observed for the C*H* groups of **1a + 1b** and their counterparts in mesobilirubin XIIIα is consistent with enantiomeric conformations wherein no new nonbonded $CH_3|CH_3$ methyl crowding is introduced.

The coupling constants seen for the ABX system of the propionic acid chain in **1a + 1b** are, mutatis mutandis, essentially the same as those seen for the ABCX system of the propionic acid chains of mesobilirubin XIIIα in $CDCl_3$ (corresponding to −14.9, 12.9, and 2.6 Hz for J_{AB}, J_{BX}, and J_{AX}, respectively, of **1a + 1b**).[8,10] These values correlate well with H_A–C–C–H_X and H_B–C–C–H_X torsion angles of ~90° and ~150° required for the propionic acid conformation dictated by the intramolecular hydrogen bonding of Figures 4 and 6. In contrast, the corresponding hydrogens of **1c** are not well resolved, due either to rapidly interconverting conformers or to a pigment conformation that affords greater mobility the the propionic acid chain. In polar solvents (DMSO-d_6) the vicinal coupling constants J_{AX}, J_{BX} are 6–8 Hz, the same as those seen in the verdin (**2**), dipyrrinone (**3**), and monopyrrole (**5**) precursors, where the propionic acid chain is not immobilized by hydrogen bonding.

^1H NMR data similar to those found for **1a + 1b** in $CDCl_3$ were found in a wide variety of solvents (Table III). Those that preserve intramolecular hydrogen bonding give spectra with similar coupling constants through the propionic acid chain and similar O*H* and N*H* chemical shits. Benzene-d_6 causes a shielding of the lactam ethyl group, apparently through orientation of the solvent's π-system over the pigment's ethyl group. In solvents that interfere with intramolecular hydrogen bonding (DMSO-d_6 and DMF-d_7) the COOH and lactam NH move strongly upfield and the pyrrole NH moves downfield, the α-CH_3 signals become shielded, possibly by moving out of the acid C=O deshielding cone, and the propionic acid chain hydrogens become more shielded, indicating changes in propionic acid rotamer conformation. Consistent with the last, the vicinal coupling constants become indistinguishable, moving to 6–8 Hz. In DMF-d_7 two species can be seen in the NMR at room temperature, one (major) apparently intramolecularly hydrogen bonded, the other not or less well intramolecularly hydrogen bonded. The ratio of the two species varies with temperature in a regular way. Assuming a two-species equilibrium, ΔH (6.1 kcal/mol) and ΔS (+1.7 cal·mol^{-1}·deg^{-1}) may be determined by plotting R ln K vs T^{-1} over the range 30–80 °C. For this solvent ~6 kcal/mol enthalpic stabilization is gained through intramolecular hydrogen bonding vs solvent stabilization of the less intramolecularly hydrogen bonded structure.

Table IV. Circular Dichroism and Ultraviolet–Visible Spectral Data from 2×10^{-5} M α,α'-Dimethylmesobilirubin XIIIα (**1a** and **1b**) at 20 °C

enantiomer	solvent	dielect const	CD			UV	
			$\Delta\epsilon_{max}$ (λ_1)	λ_2 at $\Delta\epsilon = 0$	$\Delta\epsilon_{max}$ (λ_3)	ϵ_{max}	λ nm
1a	benzene	2.3	−135 (392)	408	+252 (436)	52 200	435
1b			+134 (391)	408	−250 (436)	51 200	435
1a	carbon tetrachloride	2.2	−124 (392)	408	+259 (436)	54 000	435
1b			+120 (393)	408	−259 (436)	54 900	437
1a	carbon disulfide	2.6	−104 (404)	418	+259 (446)	56 600	440
1b			+104 (403)	418	−261 (446)	52 600	441
1a	chloroform	4.7	−133 (393)	408	+246 (436)	56 000	433
1b			+142 (391)	409	−251 (436)	52 600	433
1a	1,1,2,2-tetrachloroethane	8.2	−134 (392)	410	+227 (437)	54 400	433
1b			+136 (392)	410	−235 (438)	52 000	430
1a	dichloromethane	8.9	−128 (391)	407	+225 (434)	56 000	431
1b			+125 (390)	408	−220 (435)	53 200	430
1a	1,2-dichloroethane	10.4	−128 (390)	407	+220 (434)	51 000	432
1b			+130 (390)	408	−229 (436)	52 000	430
1a	tetrahydrofuran	7.3	−128 (391)	407	+226 (434)	52 000	432
1b			+123 (390)	407	−225 (434)	51 500	430
1a	dioxane	2.2	−129 (390)	407	+230 (434)	56 400	435
1b			+132 (389)	407	−243 (433)	54 400	432
1a	acetone	20.7	−125 (388)	405	+226 (432)	55 600	426
1b			+129 (388)	405	−230 (431)	52 600	428
1a	acetonitrile	36.2	−121 (386)	403	+214 (429)	55 200	425
1b			+124 (387)	404	−216 (430)	53 200	426
1a	1-butanol	17.1	−122 (392)	410	+196 (434)	54 000	428
1b			+129 (391)	410	−200 (432)	52 000	430
1a	1-propanol	20.1	−122 (391)	408	+187 (435)	55 000	428
1b			+125 (390)	408	−190 (434)	52 000	
1a	ethanol	24.3	−109 (387)	404	+171 (432)	61 000	429
1b			+110 (388)	404	−170 (431)	58 000	430
1a	methanol	32.6	−85 (388)	406	+141 (432)	55 700	426
1b			+85 (387)	405	−140 (422)	53 700	426
1a	pyridine	12.3	−97 (387)	408	+152 (436)	54 000	422
1b			+93 (388)	408	−148 (436)	52 000	422
1a	dimethylformamide	36.7	−59 (387)	405	+83 (431)	47 600	426
1b			+58 (385)	405	−84 (430)	48 000	429
1a	dimethyl sulfoxide	49	−9.2 (393)	406	+18.0 (428)	48 000	425
1b			+9.2 (393)	406	−18.0 (428)	48 000	425
1a	borate buffer, pH 9.0–11.0		−85 (379)	398	+125 (424)	52 000	418
1b			+87 (379)	398	−125 (424)	52 000	418
1a	phosphate buffer, pH 7.4		−84 (379)	399	+117 (425)	45 000	418
1b			+87 (379)	399	−121 (425)	46 000	418

[a] From Gordon, A. J.; Ford, R. A. *The Chemist's Companion*; Wiley: New York, 1972; pp 4–8.

Circular Dichroism Spectra and Structure. As noted above, enantiomers **1a** and **1b** give intense, bisignate circular dichroism spectra, with an opposite signed progression of Cotton effect (CE) signs. According to exciton coupling theory,[11] **1a** adopts the *P*-chirality conformer and **1b** adopts the *M*-chirality conformer. Those solvents that preserve intramolecular hydrogen bonding can be expected to favor large CEs, as shown in Table IV . Thus, nonpolar solvents such as benzene, chloroform, and tetrahydrofuran show long-wavelength $|\Delta\epsilon|$ values ranging from 225 to 260, and even in more polar aprotic solvents such as acetone and acetonitrile, very large $\Delta\epsilon$ values can be found. Alcohols such as propanol and butanol also promote comparably large $\Delta\epsilon$ values, but these decrease with lower molecular weight alcohols, such as methanol, where $|\Delta\epsilon|$ is only 50–60% of the maximum value seen in carbon tetrachloride. Apparently, both polarity and solvent hydrogen-bonding forces are at work here in destabilizing the intramolecularly hydrogen bonded pigment structure. A correlation with solvent dielectric constant is only approximate. With an increased ability by the solvent to participate in hydrogen bonding with the pigment, the $\Delta\epsilon$ values fall, as with pyridine, dimethylformamide and, most noteworthy, dimethyl sulfoxide, which is the most effective organic solvent for lowering $\Delta\epsilon$ values, apparently by interfering with intramolecular hydrogen bonding in the pigment. The thesis that dimethyl sulfoxide participates in extensive intermolecular hydrogen bonding to bilirubin, particularly between the oxygen of the S^+–O^- group and the lactam and pyrrole NH groups, has been discussed extensively,[8,22,23] and the current commonly held views is that dimethyl sulfoxide exhibits a (apparently unique) tendency to disrupt the intramolecular hydrogen bonds of bilirubin.[8,10,11,22,24] Without the benefit of intramolecular hydrogen bonding, the pigment is better able to (1) adopt other conformations, accomplished, e.g. by rotations of the pyrromethenones about torsion angles ϕ_1 and ϕ_2 (Figure 2) and/or (2) by lowering the activation energy for interconversion of the folded (but not intramolecularly hydrogen-bonded) enantiomeric conformers (only one enantiomer is shown in Figure 2), which are predicted to be the global energy minimum structures. Either (1) or (2) would lead to reduced $|\Delta\epsilon|$ values. However, since the UV–visible spectra do not differ much in dimethyl sulfoxide (where $\Delta\epsilon$ values are greatly reduced) and in, e.g., dichloromethane (where $\Delta\epsilon$ values are nearly maximal), the conformations are predicited by exciton coupling theory to be similar.

Significantly, in water at pH 9–11, where the propionic acid groups are ionized, the $\Delta\epsilon$ values are still ~50% of the maximum values—or about the same as for the pigment (acid) in methanol. These data suggest that ionization of the propionic acid groups per se does not imply extensive breaking of the intramolecular hydrogen bonds, as discussed in other work.[12,24] Rather, the reduction in $\Delta\epsilon$ values is probably due more to the hydrogen-bonding solvation and polarity effects of water—just as for the pigment dissolved in (neutral) methanol. In keeping with this

(22) Trull, F. R.; Ma, J.-S.; Landen, G. L.; Lightner, D. A. *Isr. J. Chem.* **1983**, *23*, 211–218.

(23) Gawronski, J. K.; Polonski, T.; Lightner, D. A. *Tetrahedron* **1990**, *46*, 8053–8066.

(24) Hsieh, Y.-Z.; Morris, M. D. *J. Am. Chem. Soc.* **1988**, *110*, 62–67.

(25) Grunewald, J. O.; Cullen, R.; Bredfeldt, J.; Strope, E. R. *Org. Prep. Proc. Int.* **1975**, *7*, 103–110.

thesis, the bistetra-*n*-butylammonium salts of **1a** and **1b** in chloroform exhibit the large $\Delta\epsilon$ values ($\Delta\epsilon_{438}^{max} = \pm 200$, $\Delta\epsilon_{394}^{max} = \mp 130$) characteristic of the acid in the same solvent, whereas, the bistetra-*n*-butylammonium salts in water give $\Delta\epsilon$ values ($\Delta\epsilon_{425}^{max} = \pm 125$, $\Delta\epsilon_{380}^{max} = \mp 91$) comparable to those of the sodium salts in pH 7.4–11 buffer. These results are very important for and relevant to studies of bilirubin in aqueous solvents and when bound to albumins or other proteins in water. They are consistent with a model in which the protein binds preferentially to one bilirubin enantiomer (Figure 3) through the action of salt formation between the pigment's propionic acid groups and specific amine residues on the protein.[11]

Concluding Comments

For the first time, conformational enantiomers of a bilirubin pigment have been resolved, isolated, and studied. Bilirubin itself can be predicted to be resolvable into its intramolecularly hydrogen bonded conformational enantiomers if the interconversion barrier is increased or the rates of interconversion retarded, as at sufficiently low temperatures. This has not yet been achieved. Resolution can also be expected if one conformational enantiomer is destabilized relative to the other. The latter situation can be realized through substitution of a propionic acid α-H by CH_3 to give enantiomeric α,α'-dimethylmesobilirubins XIIIα. The *R,R* and *S,S* enantiomers have been synthesized, separated, and shown to have *P* and *M* chirality of the component dipyrrinone long-wavelength-induced electric dipole transition moments. These observations underscore the considerable importance of intramolecular hydrogen bonding in bilirubins and their strong tendency to implement such hydrogen bonding. Intramolecular hydrogen bonding is found to be retained in a wide variety of solvents and plays a prominent role in even water at alkaline pH, where the carboxylic acid groups become ionized. The latter evidence is particularly relevant to on-going studies in aqueous solutions involving protein binding, conjugation, and hepatic excretion of bilirubins. Current and earlier data suggest that the resolved (*R,R*)- and (*S,S*)-α,α'-dimethylmesobilirubins XIIIα of this work may serve as powerful enantioselective agents in molecular recognition of amines and amino acids. Further studies of conformation, synthesis, and metabolism are underway for these novel pigments, their derivatives, and analogues.

Experimental Section

General Procedures. All circular dichroism spectra (CD) were recorded on a Jasco J-600 instrument and ultraviolet–visible spectra were recorded on a Cary 219 instrument or a Perkin-Elmer Model 3840 diode array instrument. Rotations were determined on a Perkin-Elmer Model 141 polarimeter. All nuclear magnetic resonance (NMR) spectra were measured on a GE QE-300 or GN-300 300-MHz instrument, and all infrared (IR) spectra were measured on a Perkin-Elmer Model 1600 FT instrument. High-resolution mass spectra (MS) were recorded by (Li) fast atom bombardment at the Midwest Center for Mass Spectrometry, University of Nebraska, Lincoln, NE. Melting points were determined on a Mel-Temp capillary apparatus and are uncorrected. Combustion analyses were carried out at Desert Analytics, Tucson, AZ.

Spectral data were obtained in spectral grade solvents (Aldrich or Fisher). Pentane-2,4-dione, ethyl acetoacetate, diethylene glycol, dimethyl sulfoxide, tetrahydrofuran, trifluoroacetic acid, 2,3-dichloro-5,6-dicyano-1,4-benzoquinone (DDQ), diphenylphosphonyl azide, hydrazine hydrate, and bromine were from Aldrich. Methanol, pyriidine, dichloromethane, and chloroform were HPLC grade from Fisher; hydrogen peroxide and zinc dust were from Fisher. Tetrahydrofuran was dried by distillation from $LiAlH_4$; dimethyl sulfoxide was dried over CaH_2 and distilled; methanol was dried (Mg, reflux) and distilled; pyridine was distilled from BaO. (*S*)-(−)-α-Methylbenzylamine ($[\alpha]^{20}_D$−39° (neat)) was used as obtained from Aldrich.

5-(Bromomethylene)-4-ethyl-3-methyl-2-oxo-1*H*-pyrrole (4). This synthetic relay component was prepared in four steps from ethyl acetoacetate and pentane-2,4-dione as described previously:[18] mp 137–139 °C (lit.[18,24] mp 138–140 °C); IR (KBr) 3353, 3107, 2967, 1699, 1640 cm^{-1}; ^1H NMR ($CDCl_3$) δ 1.14 (t, 3 H, J = 7.5 Hz), 1.86 (s, 3 H), 2.42 (q, 2 H, J = 7.5 Hz), 5.92 (s, 1 H), 7.30 (br s., 1 H) ppm; ^{13}C NMR ($CDCl_3$) δ 8.35 (q), 14.20 (q), 17.90 (t), 86.93 (d), 129.59 (s), 141.30 (s), 145. 28 (s), 171.33 (s) ppm.

Methyl 2,4-Dimethyl-5-(methoxycarbonyl)-1*H*-pyrrole-3-(2-methylpropanoate) (5). Methyl methacrylate (250 gm, 2.50 mol) was mixed with pentane-2,4-dione (250 gm, 2.50 mol) and diluted with 600 mL of 96% ethanol. To this solution was added potassium fluoride dihydrate (50 gm, 0.5 mol) (previously pulverized in a mortar), and the mixture was heated for ~7 days at reflux with stirring or until the starting materials had disappeared (as indicated by NMR on aliquots). The solvent was removed (rotary evaporator) and the potassium fluoride was removed by filtration and washed with hexane. After evaporation of the hexane, the residue was distilled three times to afford 117 gm (23%) of purified product: bp 118–121 °C (3 mmHg); IR (neat) 1730, 1698 cm^{-1}; ^1H NMR ($CDCl_3$) δ 1.15 (d, 3 H, J = 7 Hz), 2.09 and 2.12 (s, 6 H, enol and keto CH_3), 1.80–2.60 (m, 3 H, CH_2 and CH), 3.60 (s, 3 H, OCH_3), 3.70 (t, 1 H, J = 7.5 Hz), 16.85 (s, 1 H, enol OH) ppm. The material was used directly in the following step.

Ethyl acetoacetate (76 g, 0.58 mol) was dissolved in 250 mL of glacial acetic acid and treated dropwise with a solution of sodium nitrite (45 g, 0.65 mol) in 120 mL of water at a rate so that the temperature did not exceed 14 °C while efficient stirring was maintained. The solution was stirred at room temperature overnight and then the hexanoate ester above (117 g, 0.58 mol) was added in one dose followed by the addition of zinc dust (88 g, 12.34 mol) in small portions to maintain the reaction temperature at 65 °C. After the final addition, the reaction was heated at 95 °C overnight and then poured onto 3 L of ice and water. The precipitate was collected by filtration and the crude product was recrystallized to give 45 g (30%) of pure pyrrole: mp 114–116 °C; IR (film) 3284, 1734, 1652 cm^{-1}; ^1H NMR ($CDCl_3$) δ 1.09 (d, 3 H, J = 6.9 Hz), 1.32 (t, 3 H, J = 7 Hz), 2.17 (s, 3 H), 2.23 (s, 3 H), 2.309/2.395/2.414/2.442 and 2.722/2.744/2.768/2.790 (2 x dd, CH_2, AB of ABX system), 2.512/2.534/2.557/2.561 (ddg, 1 H, X of ABX system), 3.62 (s, 3 H, OCH_3), 4.27 (q, 2 H, J = 7 Hz), 8.75 (s, 1 H, NH) ppm. Anal. Calcd for $C_{14}H_{21}NO_4$ (267.3): C, 62.90; H, 7.92; N, 5.24. Found: C, 62,98; H, 8.13; N, 5.18.

Methyl 2,7,9-Trimethyl-3-ethyl-(10*H*)-dipyrrinone-8-(2-methylpropionate) (3). The diester above (5 g, 18.7 mmol) was saponified to the diacid by heating at reflux for 2 h in a solution of sodium hydroxide (4.0 g, 100 mmol) in 30 mL of 96% ethanol containing 10 mL of water and 5 g of sodium nitrate. The ethanol was removed on a rotary evaporator; then the residue was dissolved in a solution of 50 g of sodium nitrate in 10 mL of water and acidified with 60 mL of nitric acid (containing 25 g of sodium nitrate) to precipitate the diacid. The diacid was collected by filtration, washed carefully with ice water (250 mL), and dried in a vacuum desiccator over phosphorus pentoxide to give 4.2 g (100%) of pure diacid 6, which was used directly in the next step.

The diacid (4.1 g, 18.2 mmol.) and 3.95 g (18.3 mmol.) of (bromomethylene)oxopyrrole **2** were dissolved in 200 mL of methanol plus 1 mL of water, purged with nitrogen and heated at mild reflux with stirring for 6 h, during which the yellow dipyrrinone precipitated. The reaction was cooled overnight at −20 °C and the product removed by filtration and washed throughly with cold methanol. Traces of (unesterified) free acid could be removed by chromatography on a column of silica gel (CH_2Cl_2–CH_3OH, 100:1 elutes the ester), and the desired dipyrrinone ester was recrystallized from benzene–hexane 2:1 to give 3.5 g (55%) of the bright yellow product: mp 218–219 °C; IR (film) 3354, 1738, 1668, 1634 cm^{-1}; UV–visible, ϵ_{408}^{max} 35 900, ϵ_{265}^{max} 4560 ($CHCl_3$), ϵ_{412}^{max} 36 700, ϵ_{266}^{max} 4800 (CH_3OH), ϵ_{417}^{max} 33 500 (DMSO); ^1H NMR ($CDCl_3$) δ 1.12 (d, 3 H, J = 6.6 Hz), 1.16 (t, 3 H, J = 7.5 Hz), 1.93 (s, 3 H, lactam CH_3), 2.11 (s, 3 H), 2.38 (s, 3 H), 2.40–2.61 (m, 4 H), 2.80 (m, 1 H), 3.65 (s, 3 H), 6.12 (s, 1 H), 10.36 (1 H, NH), 11.29 (1 H, NH) ppm; ^{13}C NMR ($CDCl_3$) δ 8.48 (q, C_{10}), 9.74 (q, C_2^1), 11.80 (q, C_7^1), 15.01 (q, C_3^2), 16.59 (q, C_8^4), 17.97 (t, C_3^1), 28.44 (t, C_8^1), 40.70 (d, C_8^2), 51.60 (q, OCH_3), 101.19 (d, C_5), 118.12 (s, C_7), 122.41 (s, C_8), 125.06 (s, C_2), 127.09 (s, C_4), 132.27 (s, C_9), 148.37 (s, C_3), 174.14 (s, C_1), 177.09 (s, C_8^3) ppm; see Table II for numbering system. Anal. Calcd for $C_{19}H_{26}N_2O_3$ (330.4): C, 69.07; H, 7.93; N, 8.48. Found: C, 69.07; H, 7.94; N, 8.36.

α,α'-Dimethylmesobiliverdin XIIIα Dimethyl Ester 2. Dipyrrinone **3** (330 mg, 1.0 mmol) was dissolved in 100 mL of tetrahydrofuran–dimethyl sulfoxide (9:1) in a 250-mL three-neck round-bottom flask equipped with an addition funnel, nitrogen inlet and outlet, and magnetic stirrer. A solution of trifluoroacetic acid (6.0 mL) in 10 mL of argon-saturated tetrahydrofuran was added dropwise with stirring. The yellow solution turned from yellow to orange with a slight green coloration. Then a solution of DDQ (272 mg, 1.2 mmol) in 20 mL of argon-saturated tetrahydrofuran was added during 5 min while maintaining the reaction flask in an ice–water bath. The reaction turned blue. After final addition, the reaction was stirred at room temperature for 3 h with nitrogen purging.

The mixture was then transferred to a separatory funnel containing 150 mL of dichloromethane, 200 mL of water, and 40 mL of triethylamine. After shaking well, the organic layer was separated, washed with 0.2 M sodium bicarbonate until the aqueous layer was colorless, then

dried over anhydrous magnesium sulfate, and evaporated. The crude blue product was dissolved in chloroform and chromatographed on a short (4 cm) column of TLC silica gel. Elution with chloroform–2% methanol gave 210 mg (67%) of the verdin dimethyl ester, which was 99% pure by HPLC: mp 200–205 °C; IR, 3340, 1735, 1699 cm^{-1}; UV–visible, ϵ_{640}^{max} 11 200, ϵ_{369}^{max} 43 000 ($CHCl_3$); ^1H NMR ($CDCl_3$) δ 1.22 (m, 12 H), 1.82 (s, 6 H), 2.08 (s, 6 H), 2.51 (q, 4 H, J = 7.5 Hz), 2.67 (m, 4 H), 3.00 (m, 2 H), 3.67 (s, 6 H), 5.93 (s, 2 H), 6.68 (s, 1 H), 7.65 (s, H), 8.15 (s, 2 H) ppm; ^{13}C NMR ($CDCl_3$) δ 8.32 (q), 9.72 (q), 14.45 (q), 16.89 (q), 17.88 (t), 26.48 (t), 41.04 (d), 49.46 (q), 51.80 (q), 93.90 (d), 111.61 (d), 125.45 (s), 125.60 (s), 133.70 (s), 136.92 (s), 138.56 (s), 143.82 (s), 146.78 (s), 149.94 (s), 172.44 (s), 176.35 (s) ppm. Anal. Calcd for $C_{37}H_{46}N_4O_8$ (642.8): C, 69.16; H, 7.17; N, 8.72. Found: C, 68.92; H, 7.32; N, 8.74.

α,α′-Dimethylmesobilirubin XIIIα (1). To a 500-mL round-bottom flask were added 180 mL of a 1:1 tetrahydrofuran–methanol solution and 180 mL of 0.2 M sodium hydroxide solution. The mixture was purged with argon. Then 300 mg (0.47 mmol) of verdin dimethyl ester **2** and 150 mg of ascorbic acid were added to the solution and the resulting blue solution was warmed to 45 °C for 4 h under argon. After cooling, the solution was transferred to a separatory funnel containing 50 mL of 0.2 M aqueous sodium hydroxide and washed with 100 mL of dichloromethane. The organic layer was discarded and the blue aqueous layer was separated and acidified with 10% aqueous HCl and then extracted with dichloromethane (4 × 150 mL) to remove the blue verdin diacid. Evaporation of these combined organic extracts following drying over anhydrous sodium sulfate gave 245 mg (85%) of the verdin diacid, which was reduced to the rubin as follows.

In the following steps, it is important that all reactions and extractions be carried out under an argon or nitrogen atmosphere using argon- or nitrogen-saturated solvents. The verdin diacid (100 mg, 0.16 mmol) was dissolved in 100 mL of argon-saturated tetrahydrofuran–methanol (1:1), which had been dried and stirred over 4-Å molecular sieves. The solution was cooled in an ice bath and 1.0 gm (26 mmol) of $NaBH_4$ was added in four to five portions. The ice bath was removed and the solution was allowed to warm to room temperature, where it was maintained for ~30 min (or until the solution became completely yellow). The reaction was quenched by addition of 15.0 mL of argon-saturated water, and 40 mL of argon-saturated 1.0 M sodium hydroxide was added after hydrogen evolution had ceased. The solution was adjusted to pH 2–3 by adding cold 10% argon-saturated aqueous hydrochloric acid. The rubin was extracted by dichloromethane (4 × 150 mL), and the combined extracts were washed with 50% saturated aqueous sodium bicarbonate so as to afford a bright yellow organic phase. The latter was dried over anhydrous sodium sulfate, filtered, and evaporated to afford 45 mg (45%) of rubin product. HPLC indicated a 4:1 ratio of racemic to meso diastereomers, which were separated by preparative TLC on silica gel (chloroform–5% methanol irrigant). The separated diastereomers, (**1a** + **1b**) and **1c**, were each crystallized from dichloromethane–methanol (~1:2 v/v).

Racemic diastereomer 1a + 1b: mp 290 °C dec; IR (KBr) 3412, 1686, 1250 cm^{-1}; UV–visible, ϵ_{432}^{max} 52 400; ^1H NMR in Table II; ^{13}C NMR ($CDCl_3$) δ 7.95 (q, C_2^1 and C_{18}^1), 10.27 (q, C_7^1 and C_{13}^1), 14.89 (q, C_3^2 and C_{17}^2), 17.86 (t, C_3^1 and C_{17}^1), 19.68 (q, C_8^4 and C_{12}^4), 22.17 (t, C_{10}), 28.06 (t, C_8^1 and C_{12}^1), 39.17 (d, C_8^2 and C_{12}^2), 100.63 (d, C_5 and C_{15}), 119.25 (s, C_7 and C_{13}), 123.23 (s, C_8 and C_{12}), 123.91 (s, C_6 and C_{14}), 124.14 (s, C_2 and C_{18}), 128.27 (s, C_4 and C_{16}), 133.16 (s, C_9 and C_{11}), 148.42 (s, C_3 and C_{17}), 174.91 (s, C_1 and C_{19}), 182.35 (s, C_8^3 and C_{12}^3) ppm, see Table II for numbering system; high-resolution MS, 635.3592 $[M - H_2 + Li_3]^{++}$; calcd for $C_{35}H_{42}N_4O_6Li_3$, 635.3584. The exact molecular weight for $C_{35}H_{44}N_4O_6$ is 616.3261; the exact mass of ^7Li is 7.01600 and ^1H is 1.007825. Anal. Calcd for $C_{35}H_{44}N_4O_6$ (616.4): C, 68.16; H, 7.19; N, 9.08. Found: C, 67.89; H, 7.03; H, 8.97.

When the solvent is not dry, two molecules of the substance will crystallize with one molecule of water. Anal. Calcd for $C_{35}H_{44}N_4O_6 \cdot {}^1/_2H_2O$ (625.8): C, 67.18; H, 7.25; N, 8.95. Found: C, 66.92; H, 7.14; N, 8.69.

Meso diastereomer 1c: mp 245 °C dec; IR (KBr) 3411, 1665, 1272 cm^{-1}; ^1H NMR in Table II; ^{13}C NMR (DMSO-d_6) δ 8.41 (q, C_2^1 and C_{18}^1), 11.09 (q, C_7^1 and C_{13}^1), 15.18 (q, C_3^2 and C_{17}^2), 17.78 (t, C_3^1 and C_{17}^1), 22.90 (t, C_{10}), 23.70 (q, C_8^4 and C_{12}^4), 28.80 (t, C_8^1 and C_{12}^1), 38.60 (d, C_8^2 and C_{12}^2), 98.50 (d, C_5 and C_{15}), 113.10 (s, C_7 and C_{13}), 122.10 (s, C_8 and C_{12}), 122.73 (s, C_6 and C_{14}), 123.51 (s, C_2 and C_{18}), 128.87 (s, C_4 and C_{16}), 131.48 (s, C_9 and C_{11}), 147.52 (s, C_3 and C_{17}), 172.82 (s, C_1 and C_{19}), 181.00 (s, C_8^3 and C_{12}^3) ppm, see Table II for numbering system; high-resolution MS, 623.3453 $[M + Li]^{++}$; calcd for $C_{35}H_{44}N_4O_6Li$, 623.3421. The exact molecular weight for $C_{35}H_{44}N_4O_6$ is 616.3261; the exact mass of ^7Li is 7.01600. Anal. Calcd for $C_{35}H_{44}N_4O_6$ (616.4): C, 68.16; H, 7.19; N, 9.08. Found: C, 68.13; H, 7.26; N, 8.98.

Table V. Circular Dichroism Spectral Data[a] for Successive Chromatography Fractions[b] in the Resolution of α,α′-Dimethylmesobilirubin XIIIα (**1a** + **1b**) by Column Chromatography on Quinine-Bound Silica Gel

fraction	$\Delta\epsilon_{max}$ (λ_1)	λ_2 at $\Delta\epsilon = 0$	$\Delta\epsilon_{max}$ (λ_3)
1			
2	+185 (435)	408	−103 (391)
3	+129 (435)	408	−73 (391)
4	+51 (435)	408	−28 (391)
5	−15 (438)	408	+10 (391)
6	−69 (435)	408	+41 (391)
7	−96 (435)	408	+56 (391)
8	−97 (435)	408	+56 (391)

[a] Determined in ethanol-free chloroform. [b] Forty-milliliter fractions of dichloromethane eluent for the separation of 10 mg of **1a** + **1b**.

Table VI. Circular Dichroism Spectral Data for Successive Chloroform Extractions of an Aqueous Solution of Racemic α,α′-Dimethylmesobilirubin XIIIα (**1a** + **1b**) Bound to Human Serum Albumin[a]

extraction	$\Delta\epsilon_{max}$ (λ_1)	λ_2 at $\Delta\epsilon = 0$	$\Delta\epsilon_{max}$ (λ_3)
1	+125 (438)	409	−69 (391)
2	+64 (435)	409	−32 (391)
3	−7 (435)	409	+5 (391)
4	−124 (435)	409	+70 (391)
5	−251 (435)	409	+142 (391)

[a] Successive 100-mL $CHCl_3$ washings of a 100-mL solution 4.4 × 10^{-4} M in pigment and 2.2 × 10^{-4} M in albumin. The sixth washing gave pigment with the same $\Delta\epsilon$ values as the fifth.

Resolution of (*R*,*R*)- + (*S*,*S*)-α,α′-Dimethylmesobilirubin XIIIα (1a + 1b). Method 1. Chromatography. Silica gel (60–200 mesh, J. T. Baker) was dried in an oven at 100 °C over night. Fifty-two grams was heated at reflux for 24 h as a slurry in 30 mL of anhydrous toluene containing 32 g of (3-mercaptopropyl)trimethylsiloxane (Petrarch).[19] The mixture was cooled and the solid removed by filtration, washed with toluene (7 × 150 mL), and dried in air. The derivatized silica gel was suspended in chloroform and heated at reflux for 28 h with 20 g of quinine and 1.6 g of α,α′-azobisisobutyronitrile.[20] The mixture was cooled and filtered. The solid was washed with methanol to remove excess quinine completely (followed by checking the UV absorbance at 325 nm) and air-dried.

The quinine-bound silica gel was moistened in dichloromethane containing 3% acetic acid for 24 h and then slurry packed in a 2.5 cm × 21 cm chromatography column in dichloromethane. Ten milligrams of racemic pigment (**1a** + **1b**) was loaded onto the column in a small volume of dichloromethane, and the gravity chromatography was allowed to proceed using dichloromethane eluent. Forty-milliliter fractions were collected. Fraction 1 contained essentially no pigment, which eluted in fractions 2–8. After evaporation of the solvent, the CD of each fraction was run (Figure 6 and Table V).

Method 2. Extraction. The racemic mixture **1a** + **1b** (26.8 mg, 0.0435 mmol) was dissolved in 3.0 mL of 0.1 N aqueous sodium hydroxide and transferred at once to a solution of 1.5 g (0.022 mmol) of human serum albumin (HSA) in 100 mL of distilled water. The pH 9.0 solution was kept at 5–10 °C for 2 h and then extracted with eigh 100-mL aliquots of chloroform or until the washings were colorless. The first extract gave pigment (12.5 mg total) with a strongly positive long-wavelength component ($\Delta\epsilon_{435}^{max}$ = +125) of a bisignate CD. The intermediate fractions showed decreasing long-wavelength $\Delta\epsilon$ values, then sign reversal, and increasingly negative $\Delta\epsilon$ values. Extracts 5 and 6 gave 5 mg of a pigment with $\Delta\epsilon_{435}^{max}$ = −251 and a bisignate CD (Table VI). Repeated resolution of the last fractions did not lead to more negative $\Delta\epsilon$ values.

The combined pigment (12.5 mg) from the first two extracts (above) was redissolved in a solution of 680 mg of HSA in 50 mL of distilled water and extract with 50-mL portions of chloroform. The first two extracts afforded 6.2 mg of pigment with $\Delta\epsilon_{436}^{max} \simeq +250$. Repeated resolutions of these fractions did not lead to higher $\Delta\epsilon$ values. The specific rotation values for >95% resolved compound are as follows: **1a**, $[\alpha]^{25}_D$ = +4500°; **1b**, $[\alpha]^{25}_D$ = −4500° both at 5.4 × 10^{-4} M in CH_2Cl_2.

α,α′-Dimethylmesobilirubin XIIIα Bis[(*S*)-(−)-α-methylbenzyl] Amide (7a + 7b). Racemic pigment (1a + 1b) (20.0 mg, 0.032 mmol), (*S*)-(−)-methylbenzylamine (38.7 mg, 0.32 mmol), diphenylphosphoryl azide (90.0 mg, 0.32 mmol) and triethylamine (32.6 mg, 0.32 mmol) were mixed together in 2.0 mL of DMSO (dry, argon saturated). The mixture was stirred in the dark at room temperature under argon for 24 h; then it was added to 40 mL of dichloromethane. The organic layer was

washed with 2% sodium bicarbonate (4 × 40 mL), dried over anhydrous sodium sulfate, and evaporated to dryness on a Rotovap. The resulting crude product was purified by using two preparative TLC plates (20 × 20 cm, 0.5 mm thick), developed with CH_2Cl_2–MeOH–CH_3COOH (100:2:3). Two major yellow bands were separated and rechromatographed on preparative TLC under the same conditions as above to give 30% of a faster moving pigment (**7a**) and 30% of a slower moving pigment (**7b**). Each amide was crystallized from dichloromethane–hexane.

Pigment **7a**: mp 200 °C dec; $[\alpha]^{25}_D$ +3400° (*c* 2.0 × 10^{-4} M, CH_2Cl_2); IR (KBr) 3342, 3050, 2968, 1675 cm^{-1}; UV-visible, ϵ^{max}_{420} 52 000 ($CHCl_3$); ^1H NMR (DMSO) δ 0.87 (d, 6 H, *J* = 6.3 Hz), 1.04 (t, 6 H, *J* = 7.5 Hz), 1.11 (d, 6 H, *J* = 6.9 Hz), 1.73 (s, 6 H), 1.97 (s, 6 H), 2.6–2.1 (m, 10 H) 3.92 (s, 2 H), 4.52 (q, 2 H) 5.94 (s, 2 H), 7.3–7.0 (m, 10 H), 7.87 (s, 2 H), 9.80 (s, 2 H) 10.25 (s, 2 H) ppm; ^{13}C NMR (DMSO) δ 8.55 (q), 10.03 (q), 15.32 (q), 17.65 (t), 18.12 (q), 22.55 (q), 24.02 (t), 28.80 (t), 41.40 (d), 47.91 (d), 98.40 (d), 119.24 (s), 122.49 (s), 123.38 (s), 123.41 (s), 126.35 (d), 126.92 (d), 128.24 (s), 128.59 (d), 131.45 (s), 145.07 (s), 147.64 (s), 172.38 (s), 175.17 (s) ppm. Anal. Calcd for $C_{51}H_{62}N_6O_4$ (823.1): C, 74.74; H, 7.59; N, 10.21. Found: C, 74.65; H, 7.71; N, 10.28.

Pigment **7b**: mp 210 °C dec; $[\alpha]^{25}_D$ −1860° (*c* 2.0 × 10^{-4} M, CH_2Cl_2); IR (KBr) 3338, 3062, 2968, 1672 cm^{-1}; UV-visible, ϵ^{max}_{423} 51 000 ($CHCl_3$); ^1H NMR (DMSO) δ 0.92 (t, 6 H, *J* = 6.3 Hz), 1.06 (t, 6 H, *J* = 7.2 Hz), 1.12 (d, 6 H, *J* = 6.6 Hz), 1.76 (s, 6 H), 1.85 (s, 6 H), 2.5–2.0 (m, 10 H), 3.78 (s, 2 H), 4.83 (q, 2 H), 5.89 (s, 2 H), 7.3–6.9 (m, 10 H), 8.00 (s, s, 2 H), 9.88 (s, 2 H), 10.31 (s, 2 H) ppm; ^{13}C NMR (DMSO) δ 8.57 (q), 9.82 (q), 15.29 (q), 17.64 (t), 18.71 (q), 22.13 (q), 24.13 (t), 29.02 (t), 41.96 (d), 47.48 (d), 98.46 (d), 119.42 (s), 122.27 (s), 123.07 (s), 123.73 (s), 126.01 (d), 126.44 (d), 127.66 (s), 128.28 (d), 131.67 (s), 144.60 (s), 147.64 (s), 172.35 (s), 175.38 (s) ppm. Anal. Calcd for $C_{51}H_{62}N_6O_4$ (823.1): C, 74.42; H, 7.59; N, 10.21. Found: C, 74.22; H, 7.72; N, 10.09.

Acknowledgment. We thank the National Institutes of Health (Grant HD 17779) for generous support of this work. Y.M.P. was supported by a Jerry and Betty Wilson Graduate Fellowship.

Communications to the Editor

Nuclear Magnetic Resonance Crystallography: Molecular Orientational Ordering in Three Forms of Solid Methanol

Robert Tycko* and Gary Dabbagh

AT&T Bell Laboratories
Murray Hill, New Jersey 07974
Received December 5, 1990

The arrangement of molecules in crystalline solids is a principal concern of structural chemistry that is usually addressed by diffraction techniques. The applicability of X-ray and neutron diffraction is frequently limited by the need for single crystals of sufficient size and quality. In this communication, using methanol as an interesting example, we demonstrate that information about the relative orientations of nearby molecules in both polycrystalline and noncrystalline solids can be obtained from simple two-dimensional NMR measurements. Our results support one of two proposed crystal structures of α-methanol, call into question the accepted structure of β-methanol, and indicate the absence of a preferred local structure in methanol glass.

Methanol exists in two crystalline forms at ambient pressure.[1,2] The α form is stable below 157.4 K; the β form is stable between 157.4 K and the melting point (175.4 K). Methanol glass is formed by cooling the liquid at a rate of approximately 4 K/s, with a glass transition at about 115 K. In 1952, Tauer and Lipscomb proposed crystal structures based on X-ray diffraction measurements on single crystals of β-methanol and imperfect crystals of α-methanol.[3] For present purposes, the significant feature of the Tauer and Lipscomb structures is the fact that all C–O bonds in the unit cells are either parallel or antiparallel (or nearly so in the α form). Quite recently, Torrie et al. have proposed a very different structure for α-methanol, based on neutron diffraction measurements on polycrystalline samples, in which there are four nonparallel C–O bond directions in the unit cell.[4]

The anisotropic chemical shift (CSA) provides information about molecular orientations *relative to the external static magnetic field* in NMR measurements.[5,6] The methanol ^{13}C CSA tensor is characterized by principal values δ_{11} = 76 ppm, δ_{22} = 68 ppm, and δ_{33} = 7 ppm (relative to TMS). Separated-local-field

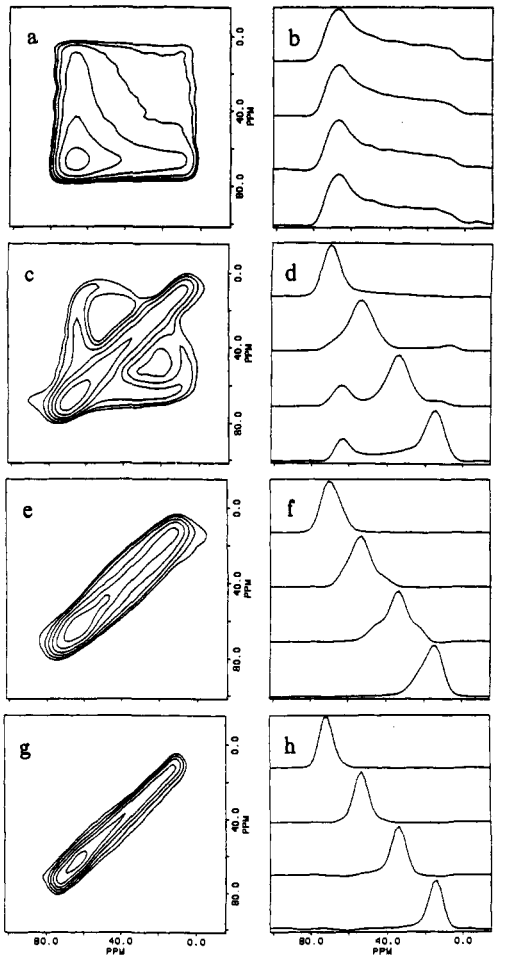

Figure 1. Two-dimensional ^{13}C NMR (100.5 MHz) exchange spectra of solid $^{13}CH_3OH$: (a,b) glass at 103 K; (c,d) α form at 133 K; (e,f) β form at 168 K; (g,h) β form at 168 K, 4.5% $^{13}CH_3OH$/95.5% CH_3OH. Spectra are represented as contour plots (a, c, e, and g) and as vertical cross sections at 73, 53, 34, and 14 ppm (b, d, f, and h).

(1) Parks, G. S. *J. Am. Chem. Soc.* **1925**, *47*, 338–345.
(2) Kelley, K. K. *J. Am. Chem. Soc.* **1929**, *51*, 180–187.
(3) Tauer, K. J.; Lipscomb, W. N. *Acta Crystallogr.* **1952**, *5*, 606–612.
(4) Torrie, B. H.; Weng, S.-X.; Powell, B. M. *Mol. Phys.* **1989**, *67*, 575–581.
(5) Haeberlen, U. *High Resolution NMR in Solids: Selective Averaging*; Academic Press: New York, 1976.
(6) Mehring, M. *Principles of High Resolution NMR in Solids*; Springer-Verlag: New York, 1983.

0002-7863/91/1513-3592$02.50/0 © 1991 American Chemical Society